Adaptive optics system with a correlation detector of image displacements

L.V. Antoshkin, N.N. Botygina, O.N. Emaleev, P.G. Kovadlo,* P.A. Konyaev, V.P. Lukin, A.I. Petrov, and A.P. Yankov

Institute of Atmospheric Optics,
Siberian Branch of the Russian Academy of Sciences, Tomsk
** Institute of Solar-Terrestrial Physics,*
Siberian Branch of the Russian Academy of Sciences, Irkutsk

Received June 11, 2002

The results of testing adaptive optics system with a correlation detector of image displacements are discussed. The adaptive optics system consists of the following basic components: a tip-tilt mirror with piezoelectric drive, drive controller (RS-232 interface), computer (Pentium III, 550 MHz), DALSA video camera (256 × 256 pixel, 8 bit ADC, 203 frames/s), video camera controller (ISA bus), software (specially developed). The tests were conducted at the Big Solar Vacuum Telescope of the Institute of Solar-Terrestrial Physics (the Baikal Astrophysical Observatory). The adaptive optics system stabilized the position of a solar disk image fragment. The relative error of the control was, on the average, about 50%.

Introduction

When studying various parts of the Sun disk by spectroscopic methods, it is necessary to stabilize different structures of the solar disk image on the spectrograph's entrance slit. For stabilizing a fragment of a granulation pattern in solar telescopes, adaptive optics systems with a correlation detector of image displacement (correlation trackers) are used; see, for example, Ref. 1.

As a part of our works[2,3] on the development of a correlation tracker for the Big Solar Vacuum Telescope (BSVT) of the Baikal Astrophysical Observatory, we have made and tested a laboratory mock-up of such a system. The correlation detector[4] was operated at different image structures close in the angular scale and contrast to actual images of a solar telescope.

In this paper, we present the results of testing the adaptive optics system with the correlation detector of image displacements in the Big Solar Vacuum Telescope.

Functional diagram of the setup

Optical arrangement of the experimental setup at the BSVT is shown in Fig. 1. With the beam-turning mirror *2*, a part of radiation forming the sun image is directed into the correlation tracker. The spherical mirror *3* and the telescope objective *1* form a telescopic system with the tip-tilt mirror *4* in the output pupil. The mirrors *3* and *4* transfer the image from the plane near the focus F_1 into the plane near F_2. The image is first captured with the video camera *6* and then entered via specially developed controller into a computer *7*, which calculates image displacements and generates control signals. The control signals come through the RS-232 drive controller to the piezoelectric drive[5] of the tip-tilt mirror *4*.

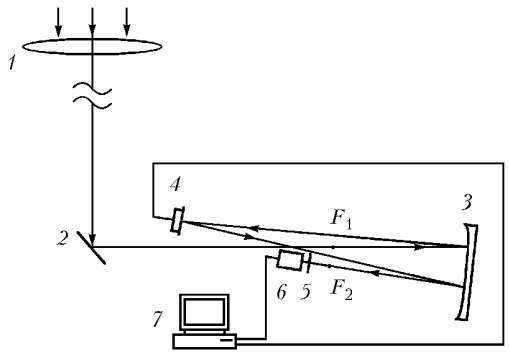

Fig. 1. Optical arrangement of the setup: telescope objective *1* (D = 760 mm, F = 40 m), beam-turning mirror *2*, spherical mirror *3* (F = 4 m), tip-tilt mirror *4*, filters *5*, DALSA video camera *6* (256 × 256 pixels, 8-bit ADC, 203 frames/s); computer *7* (Pentium III, 550 MHz, ASUS AGP-V3800 Pro/TV video display card).

For operation of the correlation tracker, we have developed specialized computer codes to support the following functional features:

– displaying the image on a computer monitor;

– selecting the operation mode: (a) image browsing, (b) measurement, (c) tracking;

– viewing the brightness distribution in a selected cross section;

– selecting the analysis window;

– specifying system parameters and the number of measurement cycles;

– calculating image displacement coordinates;

– generating control signals;

0235-6880/02/11 934-04 $02.00

– reading the statistical characteristic of the correlation detector and the correlation tracker;

– saving: (a) the image, the system operates with, (b) measurement conditions, (c) calculated coordinates of the image displacement, (d) control signal.

Measurement technique and results

The correlation technique of measuring the image fragment displacement consists in the following: a reference frame is stored and the mutual correlation function of the brightness distribution of the reference and current frames is calculated. The position of the peak of the mutual correlation function determines the coordinates of the displacement of a current frame with respect to the reference one.

For calculating the correlation, we used the Fast Fourier Transform Mixed Radix algorithm operating in the 16-bit floating-point arithmetic.

The correlation tracker for stabilization of a sun image fragment was tested at the BSVT under clear sky conditions in August of 2001. As a tracking object, we used various structures within a finite image fragment (granulation pattern, images of sunspots and pores) having different contrast.

The contrast of the granulation pattern under the experimental conditions was, on the average, 1.5–2%. Therefore, it was difficult to use a fragment of the granulation pattern as an object for tracking. This is connected with the fact that, as an image is captured with a video camera equipped with an 8-bit ADC, the modulation depth of the signal insignificantly exceeds the modulation connected with the camera noise. In this case, the correlation detector operates by the noise modulation, and this leads to the measurement error and decreases the efficiency of the image stabilization. The brightness distribution of the granulation pattern is shown in Fig. 2.

The image was recorded directly with the CCD of the video camera placed at the telescope focal plane. The exposure time was roughly 5 ms. The radiation flux was attenuated by neutral filters and an interference filter at the wavelength of 0.589 μm. The camera's field of view was 20.5 × 20.5 arc. sec, and the resolution was about 0.08 arc. sec. The granulation area near a pore was recorded. The telescope was adjusted for sharpness against a pore edge within the camera's field of view. The brightness distribution is shown as Y = const cross sections with the step equal to one pixel of the CCD array.

One cross section is shown separately in Fig. 2*b* on the scale convenient for consideration of the fine structure. The image obtained was used in the model experiments for analysis of correlation detector operation. The model studies showed that for the efficient operation of the correlation sensor with the image fragment in the form of the granulation pattern having the contrast of 1.5–2% we need a lower-noise video camera with a wider dynamic range, i.e., an ADC with higher bit capacity.

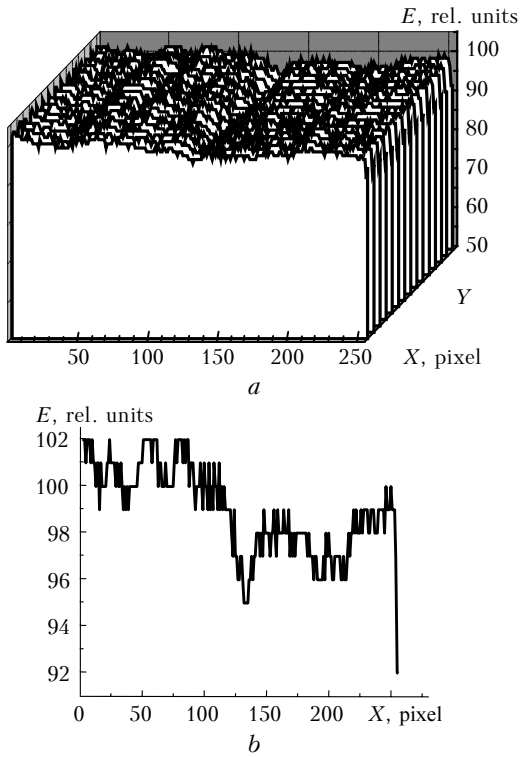

Fig. 2. Brightness distribution in the granulation pattern. Image fragment corresponding to the field of view of 20.5×1.2 arc. sec (*a*), a cross section (*b*). One pixel = 0.08 arc. sec.

To test the correlation tracer with its maximum possible speed and the detector resolution up to 1 arc. sec, objects for tracking that would allow using a small analysis window were selected on the solar disc image. In the majority of cases, the analysis window was 24 × 16 pixels corresponding to the tracker's field of view equal to 24.80 × 16.50 arc. sec. At the analysis window of 24 × 16 pixels, the duration of measurement–control cycle was 17.8 ms. The tracker operated with images of small sunspots and pores. The image contrast varied from 6 to 40%. The contrast of a sunspot image was determined as follows:

$$K = (E_{\max} - E_{\min}) \;/\; (E_{\max} + E_{\min}),$$

where $E_{\max}$ and $E_{\min}$ are the maximum and minimum brightness in the analysis window.

To determine the feedback coefficient of the correlation tracker, the statistical characteristic of the tracker with the open-loop control was first determined. For this purpose, a point source was placed at the telescope focus F_1 (see Fig. 1), the control signal was sent from the computer to the tip-tilt mirror *4*, and displacement of the point source image at the focus F_2 was measured by the correlation detector of the image displacement.

The tracker operation was evaluated using two parameters:

– the relative tracking error: σ_{er}/σ_c, where σ_{er} and σ_c are the rms deviations of the error and control signals;

– the efficiency of suppression of the spectral components of the image jitter:

$$|S(f)|^2/|S(f)_{er}|^2,$$

where $|S(f)|^2$ and $|S(f)_{er}|^2$ are the spectral power densities of image displacement signals at open-loop control and residual image displacement signals in the tracking mode.

To illustrate the tracker operation, we present the results obtained at stabilization of the position of the image fragment marked by a frame in Fig. 3. The object for tracking was the sunspot image with the size of 9 arc. sec at the half-maximum level of the brightness modulation depth. The image contrast was 8%.

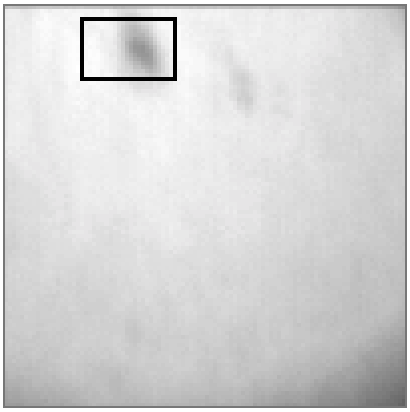

Fig. 3. Fragment of the solar disc image (the image contrast is increased).

In all cases when a sunspot completely fell within the reference frame, the relative tracking error was, on the average, 50%. Figure 4 shows the power spectrum of the image jitter signal at open-loop control. Figure 5 depicts the power spectra of the error and control signals and their comparison. The spectra shown in Figs. 4 and 5 were obtained from 17.8-s long realizations recorded in measurement and tracking mode sequentially with the interval of several seconds. The reading frequency, f_s, was equal to 56.0 Hz. The efficiency of image jitter suppression at different frequencies is shown in Fig. 6, from which one can see that the efficiency of the image stabilization system is higher than unity in the frequency range from 0 to 11.0 Hz.

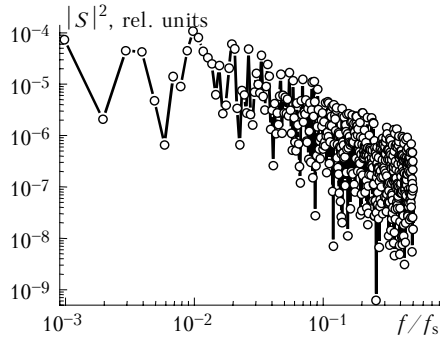

Fig. 4. Power spectrum of the image jitter signal.

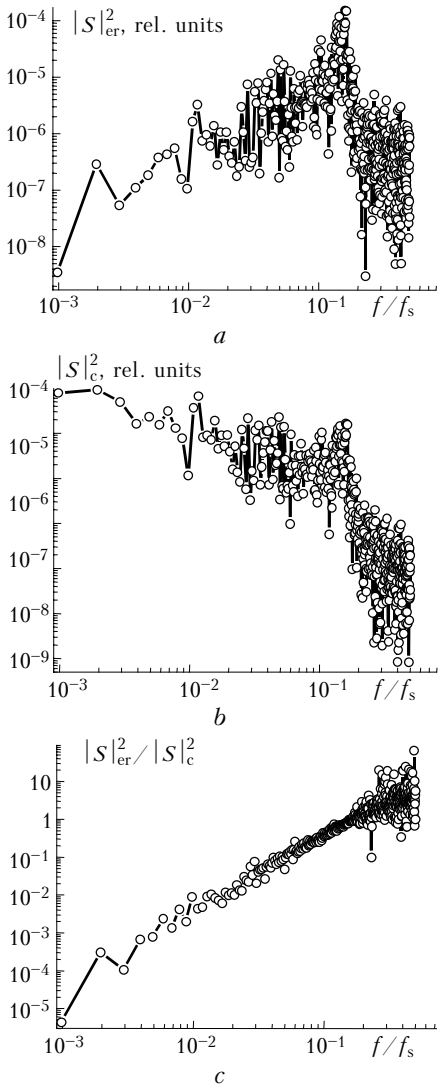

Fig. 5. Power spectra of error (*a*) and control (*b*) signals and their comparison (*c*).

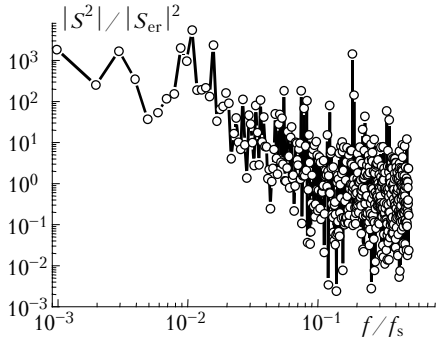

Fig. 6. Frequency dependence of the efficiency of jitter suppression.

To understand what causes the tracking error, we entered an image, the real detector dealt with, into the computer model of the correlation detector of image displacement and drew the position characteristic of the detector. Thus, we have revealed the possibility of calculating in principle the displacement of an actual

image recorded under conditions of a particular realization at the given initial position and size of the analysis window using the correlation method. It turned out that when a sunspot completely fell within the reference frame, the position characteristic of the detector was linear. If only a sunspot part was in the reference frame, the correlation detector worked incorrectly. Therefore, to evaluate the operation speed of an actual system, the processing involved only those realizations, in which the sunspot completely fell within the reference frame. In this case, the tracking error of the actual system is not caused by the inherent disadvantages of the method, but by the dynamic characteristics of the system and, in the first turn, by noise and low operation speed, as well as by the change in the image brightness distribution during sampling.

Conclusion

The adaptive optics system with the correlation detector of image displacements (correlation tracker) was tested at the BSVT, and the tests showed that it compensates for jitter of images of small sunspots and pores at the frequencies below 11 Hz. To improve the image stabilization, it is needed to increase the spatial resolution of the correlation detector and significantly increase the system speed (by an order of magnitude and higher). To do this, it is necessary to increase the analysis window and significantly shorten the measurement–control cycle. This will be possible if we replace some system elements with higher-speed ones. Besides, for the correlation tracker to operate with any fragments of the solar disk image, in particular, with the granulation pattern, a video camera with a wider dynamic range is needed.

Thus, the tests conducted have allowed us to determine the capabilities of the developed correlation tracker at operation with various fragments of the solar disk image and to draw up the ways for its further improvement.

Acknowledgments

This work was partly supported by the Russian Foundation for Basic Research (Project No. 00–02–17489) and SB RAS (Combined Integration Project No. 6 “Adaptive solar telescope”).

References

1. O. von der Luhe, A.L. Widener, Th. Rimmele, G. Spence, R.B. Dunn, and P. Wiborg, Astron. Astrophys. **224**, 351–360 (1989).
2. V.P. Lukin, B.V. Fortes, L.V. Antoshkin, N.N. Botygina, O.N. Emaleev, L.N. Lavrinova, A.I. Petrov, A.P. Yankov, A.V. Bulatov, P.G. Kovadlo, and N.M. Firstova, Atmos. Oceanic Opt. **12**, No. 12, 1107–1110 (1999).
3. L.V. Antoshkin, N.N. Botygina, O.N. Emaleev, L.N. Lavrinova, V.P. Lukin, A.I. Petrov, B.V. Fortes, and A.P. Yankov, Atmos. Oceanic Opt. **13**, No. 4, 389–392 (2000).
4. P.A. Konyaev, V.P. Lukin, N.N. Botygina, and O.N. Emaleev, in: *Proc. of the VIII Joint International Symposium on Atmospheric and Ocean Optics. Atmospheric Physics* (Tomsk, 2001), p. 118.
5. L.V. Antoshkin, N.N. Botygina, O.N. Emaleev, P.A. Konyaev, V.P. Lukin, and A.P. Yankov, Prib. Tekh. Eksp., No. 1, 144–146 (2002).